

BERNARDO COCKBURN

CHI-WANG SHU

**The Runge-Kutta local projection P^1 -
discontinuous-Galerkin finite element method
for scalar conservation laws**

M2AN. Mathematical modelling and numerical analysis - Modélisation mathématique et analyse numérique, tome 25, n° 3 (1991), p. 337-361

http://www.numdam.org/item?id=M2AN_1991__25_3_337_0

© AFCET, 1991, tous droits réservés.

L'accès aux archives de la revue « M2AN. Mathematical modelling and numerical analysis - Modélisation mathématique et analyse numérique » implique l'accord avec les conditions générales d'utilisation (<http://www.numdam.org/conditions>). Toute utilisation commerciale ou impression systématique est constitutive d'une infraction pénale. Toute copie ou impression de ce fichier doit contenir la présente mention de copyright.

NUMDAM

Article numérisé dans le cadre du programme
Numérisation de documents anciens mathématiques
<http://www.numdam.org/>

THE RUNGE-KUTTA LOCAL PROJECTION P¹-DISCONTINUOUS-GALERKIN FINITE ELEMENT METHOD FOR SCALAR CONSERVATION LAWS (*)

Bernardo COCKBURN ⁽¹⁾ and Chi-Wang SHU ⁽²⁾

Communicated by J DOUGLAS

Abstract — In this work we introduce and analyze the model scheme of a new class of methods devised for numerically solving hyperbolic conservation laws. The construction of the scheme is based on a Discontinuous Galerkin finite element space-discretization, combined suitably with a high-order accurate total variation diminishing Runge-Kutta time-discretization, and a local projection which enforces the global stability of the scheme. The resulting scheme verifies a maximum principle, is total variation bounded in the means, linearly stable for $CFL \in [0, 1/3]$, and formally uniformly second-order accurate in time and space. Moreover, it converges to a weak solution. We give extensive numerical evidence that the scheme does converge to the entropy solution, and that the order of convergence away from singularities is optimal, i.e., equal to 2 in the norm of $L^\infty(L^\infty_{loc})$.

Resumé — Dans ce travail nous introduisons et analysons le schéma modèle d'une nouvelle classe de méthodes pour résoudre numériquement les lois de conservation hyperboliques. La construction du schéma est basée sur une discrétisation en espace par éléments finis discontinus et sur une discrétisation en temps par un schéma de Runge Kutta d'ordre élevé à variation totale décroissante. Le schéma obtenu satisfait un principe du maximum, est à variation totale bornée en moyenne, linéairement stable pour $CFL \in [0, 1/3]$, et formellement du second ordre en temps et en espace. De plus il converge vers une solution faible. Nous montrons numériquement que le schéma converge vers la solution entropique, et que l'ordre de convergence en dehors des singularités est optimal, c'est-à-dire égal à deux pour la norme de $L^\infty(L^\infty_{loc})$.

(*) Received December 1989

⁽¹⁾ Institute for Mathematics and its Applications, University of Minnesota, 514 Vincent Hall, Minneapolis, Minnesota 55455. Present address: School of Mathematics, University of Minnesota, 127 Vincent Hall, Minneapolis, Minnesota 55455.

⁽²⁾ Institute for Mathematics and its Applications, University of Minnesota, 514 Vincent Hall, Minneapolis, Minnesota 55455. Present address: Division of Applied Mathematics, Brown University, Providence, RI 02912.

1. INTRODUCTION

This is the first of a series of papers in which we introduce, analyze and test a new class of explicit methods devised for numerically solving the conservation law :

$$(1.1) \quad \begin{aligned} \partial_t u + \operatorname{div} f(u) &= 0, \quad \text{in } (0, T) \times \mathcal{C}, \\ u(t=0) &= u_0, \quad \text{on } \mathcal{C}, \end{aligned}$$

where $\mathcal{C} \subset \mathbb{R}^d$, u is a m -valued function, and any real combination of the Jacobian matrices $\sum_{i=1}^d \xi_i \frac{\partial f_i}{\partial u}$ has m real eigenvalues and a complete set of eigenvectors. The schemes of this new class are devised to combine the ability of the finite element methods to handle complicated geometries and boundary conditions, with the uniform high-order accuracy in time of Runge-Kutta methods, while verifying maximum principles, and achieving convergence to a weak solution.

In this paper we shall restrict ourselves to the one dimensional scalar case ($d = m = 1$) with periodic boundary conditions (i.e., \mathcal{C} is a circle). The function u_0 will be taken in $BV(\mathcal{C})$, the set of functions on \mathcal{C} of finite bounded variation. In this setting we shall define and study our model scheme, the so-called Runge-Kutta Local-Projection Discontinuous Galerkin P^1 ($RK\Lambda PP^1$) method. We have chosen to work in a periodic setting in order to avoid the problem of the numerical treatment of the boundary conditions. This setting might appear to be too restrictive, however, it allows us to simplify the presentation and focus on the essential ingredients of the method. Moreover, the principles on which the model scheme is constructed can be extended to the cases in which $d, m > 1$ and \mathcal{C} is an arbitrary subset of \mathbb{R}^d . This extension will be developed in the series of papers we initiate with this work.

The $RK\Lambda PP^1$ -method is an explicit conservative scheme that displays a convenient local maximum principle and has the property of being total variation bounded in the means (TVBM). At the same time, it is linearly stable under the mild condition $CFL \leq 1/3$, and formally second-order accurate in the $L^\infty(0, T; L^\infty_{loc})$ -norm even in the presence of extrema and sonic points. We prove the convergence in $L^\infty(0, T; L^1(\mathcal{C}))$ of a subsequence of the sequence of approximate solutions generated by the method to a weak solution of (1.1). We also give extensive numerical evidence that the scheme does converge to the entropy solution — the only weak solution with physically relevant meaning — and that the order of convergence away from singularities is optimal; i.e., equal to 2 in the $L^\infty(0, T; L^\infty_{loc})$ -norm.

Historically, the $RK\Lambda PP^1$ -method has been originated from two sources.

One of them is the $\Lambda\Pi P^0P^1$ -scheme for scalar conservation laws introduced and analyzed recently by Chavent and Cockburn [3]. In this finite element method the approximate solution is piecewise-constant in time and piecewise-linear in space. It is determined by using the weak formulation of the explicit Discontinuous Galerkin Method, introduced by Chavent and Salzano in [4], and a local projection based on the monotonicity-preserving local projections introduced by Van Leer [10]. This local projection, the $\Lambda\Pi_h$ -projection, guarantees a local maximum principle and the TVDM (total variation diminishing in the means) property. It was proven that these properties, together with the conservativity of the scheme, ensure the convergence of a subsequence to a weak solution, and extensive numerical evidence showing that the scheme converges to the entropy solution at a rate of $O(h)$ in the norm of $L^\infty(0, T; L^1(\mathcal{G}))$ (even in the presence of discontinuities) was given. Unfortunately, any attempt to obtain higher-order accurate extensions of the $\Lambda\Pi P^0P^1$ -scheme staying in the framework of this finite element technique leads naturally to implicit schemes. And it is very well known that implicit schemes do not perform as well as explicit ones for this kind of problems (on this respect we want to bring the reader's attention to the explicit-implicit version of the Piecewise Parabolic Method-scheme; see [7]).

The other source is the efficient Runge-Kutta techniques that enforce total variation diminishing (TVD) high-order accurate time-discretizations of scalar conservation laws introduced by Shu and Osher [12]. They use the method of lines; i.e., first, they discretize the equation in space by using a finite difference non-oscillatory technique. The equation satisfied by the approximate solution can be then written in ODE form: $\frac{d}{dt} u_h = L_h(u_h)$. Then the latter equation is discretized in time by using a suitably chosen Runge-Kutta technique. This is done in such a way that the local truncation error of the resulting scheme is formally $O((\Delta t)^r + h^r)$ whenever $L_h(u)$ approximates $-\partial_x f(u)$ with an $O(h^r)$ error; see [12]. These Runge-Kutta techniques are essentially ODE-discretization techniques which do not increase the total variation of the spatial part, and so are absolutely independent of the type of discretization used in space as well as of the dimension of the space variables. As long as the spatial dimension is bigger than one, finite difference approximations of L_h are difficult to obtain when the domain has a complicated geometry. However, this is not the case if a finite element discretization technique is used. It is then very natural to combine the above mentioned Runge-Kutta technique with the finite element space discretization of the P^0P^1 -scheme. The $RK\Lambda\Pi P^1$ -scheme is a realization of this idea. It is obtained in three steps:

- 1) the conservation law is discretized in space by using the explicit discontinuous-Galerkin finite element used by Chavent and Salzano [4].

An ODE of the form $\frac{d}{dt} u_h = L_h(u_h)$ is thus obtained ;

- 2) the latter ODE is discretized in time by using a suitably chosen TVD Runge-Kutta technique as indicated by Shu and Osher [12] ;
- 3) a TVBM extension of the TVDM $\Lambda\Pi_h$ -projection introduced by Chavent and Cockburn [3] is then used in order to render the scheme stable and the sequence of approximate solutions compact in $L^\infty(0, T; L^1(\mathcal{C}))$, without compromising the accuracy of the method.

An outline of the paper follows. In § 2 the discretization of the scalar conservation law in space is obtained. In § 3 the time discretization is constructed. In § 4 the $\Lambda\Pi_h$ -projection is studied. In § 5 the $RK\Lambda\Pi P^1$ -method is defined and its stability, formal accuracy and convergence properties are proven. In § 6 numerical results are shown. Some concluding remarks are given in § 7.

2. THE SPACE-DISCRETIZATION

First, let us introduce some notation. As usual, the set $\{x_{i+1/2}\}_{i=0, \dots, nx-1}$ is a partition of the circle \mathcal{C} . Note that $x_{1/2} = 0$. For commodity, we define $x_{nx+1/2} = x_{1/2}$. We define $\Delta x_i = x_{i+1/2} - x_{i-1/2}$, denote by I_i the interval $(x_{i-1/2}, x_{i+1/2})$, and set $h = \sup_i \{\Delta x_i\}$. By $I(a_1, \dots, a_m)$

we shall denote the closed interval $[\min \{a_1, \dots, a_m\}, \max \{a_1, \dots, a_m\}]$.

To discretize the equation (1.1) in space we use the Discontinuous Galerkin method as used in [3, 4]. We proceed in two steps. First, we introduce the finite dimensional space V_h . A function u_h is said to belong to $V_h(\mathcal{C})$ if $u_h \in BV(\mathcal{C}) \cap L^1(\mathcal{C})$ and :

(2.1a) On each element $I_i \subset \mathcal{C}$, u_h is linear : $u_h|_{I_i} \in P^1(I_i)$; i.e.,

$$u_h(x) = \bar{u}_i^n \varphi^0(s) + \tilde{u}_i^n \varphi^1(s), \quad x \in I_i,$$

where

$$\varphi^0(s) = 1, \text{ and } \varphi^1(s) = 2s, \quad \forall s = (x - x_i)/\Delta x_i \in \left(-\frac{1}{2}, \frac{1}{2}\right).$$

(2.1b) The *trace* of u_h in each ∂I_i is chosen as follows :

$$\begin{aligned} u_h(x_{i+1/2}) &= \xi_{h,i+1/2}, \\ f(\xi_{h,i+1/2}) &= f^G(u_h(x_{i+1/2} + 0), u_h(x_{i+1/2} - 0)), \end{aligned}$$

where f^G denotes the Godunov flux associated to the function f .

The Godunov flux associated to the function h , h^G , is a consistent two-point numerical flux, i.e., $h^G(w, w) = h(w)$, defined by

$$(2.2) \quad \begin{aligned} h^G(w, v) &= h(\xi), \quad \text{with } \xi \in I(w, v): \\ (h(\xi) - h(c)) \cdot \text{sign}(w - v) &\leq 0, \quad \forall c \in I(w, v). \end{aligned}$$

See Osher [9], and Brenier and Osher [1] for further details. Note that :

$$(2.3) \quad \begin{aligned} \bar{u}_i^n &= \int_{I_i} \varphi^0(s(x)) u_h(x) dx / \Delta x_i = \int_{I_i} u_h(x) dx / \Delta x_i, \\ \tilde{u}_i^n &= 3 \int_{I_i} \varphi^1(s(x)) u_h(x) dx / \Delta x_i = 6 \int_{I_i} (x - x_i) u_h(x) dx / (\Delta x_i)^2. \end{aligned}$$

Now, set $\mathbb{V}_h(\mathcal{C}) = \{v_h : [0, T] \times \mathcal{C} \rightarrow \mathbb{R} \mid v_h(t) \in V_h(\mathcal{C}), \forall t \in [0, T]\}$. The approximate solution, u_h , will be taken in the space $\mathbb{V}_h(\mathcal{C})$, and will be determined as the unique solution of a weak formulation that we derive as follows. Multiply (1.1) by φ , integrate over the domain I_i , and formally integrate by parts to get :

$$(2.4) \quad \begin{aligned} &\int_{I_i} \partial_t u \cdot \varphi \\ &- \int_{I_i} f(u) \cdot \partial_x \varphi + \int_{\partial I_i} f(u) \cdot \varphi \cdot n_x = 0, \quad \forall \varphi \in C^1(I_i), \end{aligned}$$

where n_x is the outward unit normal to ∂I_i . In order to compute numerically integrals over I_i use the quadrature rule :

$$(2.5) \quad \int_{I_i} \psi \sim \sum_{l=1}^L \omega_l \psi(x_{i,l}) \Delta x_i,$$

where $x_{i,l} = x_i + \theta_l \Delta x_i$, $l = 1, \dots, L$. In this way, $u_h \in \mathbb{V}_h$ will be determined as the unique solution of :

$$(2.6) \quad \begin{aligned} &\forall t \in (0, T), \quad \forall \varphi \in P^1(I_i): \\ &\int_{I_i} \partial_t u_h \cdot \varphi - \sum_{l=1}^L \omega_l \cdot f(u_h((x_{i,l}))) \cdot \partial_x \varphi(x_{i,l}) \Delta x_i + \int_{\partial I_i} f(\xi_h) \cdot \varphi \cdot n_x = 0, \end{aligned}$$

satisfying the initial condition $u_h(t=0) = \mathbb{P}_h(u_h)$, where \mathbb{P}_h is the L^2 -projection into the space $V_h(\mathcal{C})$. Roughly speaking, by using the variational formulation based on (2.4) we force the approximate solution

u_h to be an approximation to a weak solution of (1.1); and by using the definition of its trace as in (2.1b) we are forcing u_h to behave like the entropy solution of (1.1).

We can characterize our approximate solution u_h as the unique solution of an ODE initial-value problem as follows.

PROPOSITION 2.1: *Let u_h be the approximate solution defined above. Then u_h is the unique solution of the initial-value problem:*

$$(2.7a) \quad \frac{d}{dt} u_h(t) = L_h(u_h(t)), \quad \text{in } (0, T),$$

$$u_h(t=0) = u_{0,h}$$

where the operator L_h is given by

$$(2.7b) \quad \begin{aligned} L_h(u) : BV(\mathcal{C}) \cap L^1(\mathcal{C}) &\rightarrow V_h(\mathcal{C}), \\ u &\mapsto w_h, \end{aligned}$$

and the degrees of freedom of w_h are given by

$$(2.7c) \quad \begin{aligned} \bar{w}_i &= - (f^G(u(x_{i+1/2}^+), u(x_{i+1/2}^-)) - f^G(u(x_{i-1/2}^+), u(x_{i-1/2}^-))) / \Delta x_i, \\ \bar{w}_i &= -3((f^G(u(x_{i+1/2}^+), u(x_{i+1/2}^-)) + f^G(u(x_{i-1/2}^+), u(x_{i-1/2}^-))) \\ &\quad - 2 \left\{ \sum_{l=1}^L \omega_l \cdot f(u(x_{i,l})) \right\}) / \Delta x_i. \end{aligned}$$

Compare this with equations (2.7) in [3].

Proof: Assuming that (2.7c) is correct, the operator L_h is Lipschitz and so the initial-value problem (2.7a)-(2.7b) has a unique solution. Now, let us prove (2.7c). By the inversion formulae (2.3) we have:

$$\begin{aligned} \bar{w}_i &= \int_{I_i} w_h(x) dx / \Delta x_i \\ &= \int_{I_i} L_h(u_h)(x) dx / \Delta x_i \\ &= \int_{I_i} \frac{d}{dt} u_h(x) dx / \Delta x_i \\ &= - \int_{\partial I_i} f(\xi_h) n_x, \quad (\text{set } \varphi \equiv 1 \text{ in (2.6)}), \\ &= - (f^G(u(x_{i+1/2}^+), u(x_{i+1/2}^-)) - f^G(u(x_{i-1/2}^+), u(x_{i-1/2}^-))) / \Delta x_i. \end{aligned}$$

Similarly, from (2.3),

$$\begin{aligned}
 \tilde{w}_i &= 6 \int_{I_i} (x - x_i) w_h(x) dx / (\Delta x_i)^2 \\
 &= 6 \int_{I_i} (x - x_i) L_h(u_h)(x) dx / (\Delta x_i)^2 \\
 &= 6 \int_{I_i} (x - x_i) \frac{d}{dt} u_h(x) dx / (\Delta x_i)^2 \\
 &= \sum_{l=1}^L \omega_l \cdot f(u_h(x_{i,l})) \cdot [6/(\Delta x_i)^2] \Delta x_i - \int_{\partial I_i} f(\xi_h) [3/\Delta x_i] n_x, \\
 &\quad (\text{set } \varphi(x) \equiv 6(x - x_i)/(\Delta x_i)^2 \text{ in (2.6)}) , \\
 &= -3((f^G(u(x_{i+1/2}^+), u(x_{i+1/2}^-)) + f^G(u(x_{i-1/2}^+), u(x_{i-1/2}^-))) \\
 &\quad - 2 \left\{ \sum_{l=1}^L \omega_l \cdot f(u(x_{i,l})) \right\}) / \Delta x_i .
 \end{aligned}$$

This completes the proof. \square

The operator $L_h(\cdot)$ is the discretization by the discontinuous Galerkin method under consideration of the nonlinear operator $-\partial_x f(\cdot)$. If the function u is continuous, and the quadrature rule (2.5) used in (2.7c) is exact, then it is easy to see that $L_h(u)$ is nothing but $\mathbb{P}_h(-\partial_x f(u))$ — the L^2 -projection of $-\partial_x f(u)$ on the finite element space $V_h(\mathcal{G})$. In fact, $L_h(\cdot)$ is a second-order approximation of $-\partial_x f(\cdot)$, as we prove next.

PROPOSITION 2.2: *Assume that u is an element of $W^{3,\infty}(\mathcal{G})$, that f' belongs to $W^{2,\infty}(C(u))$, where $C(u)$ denotes the range of u , and that the quadrature rule (2.5) is exact for polynomials of degree two. Then, there is a constant C such that*

$$\| -\partial_x f(u) - L_h(u) \|_{L^\infty(\mathcal{G})} \leq Ch^2 \| \partial_x^3 f(u) \|_{L^\infty(\mathcal{G})} .$$

Proof: For $x \in I_i$ we have

$$-\partial_x f(u(x)) - L_h(u)(x) = e_1(x) + e_2(x) ,$$

where

$$\begin{aligned}
 e_1(x) &= -\partial_x f(u(x)) - \mathbb{P}_h(-\partial_x f(u))(x) , \\
 e_2(x) &= \mathbb{P}_h(-\partial_x f(u))(x) - L_h(u)(x) .
 \end{aligned}$$

Set $v_h = \mathbb{P}_h(-\partial_x f(u))$. Then, proceeding as in the proof of the preceding

Proposition, and taking into account the continuity of u , we obtain :

$$\begin{aligned}\bar{v}_i &= - (f(u(x_{i+1/2})) - f(u(x_{i-1/2}))) / \Delta x_i, \\ \tilde{v}_i &= - 3 \left(f(u(x_{i+1/2})) + f(u(x_{i-1/2})) - 2 \left\{ \int_{I_i} f(u(x)) dx \right\} / \Delta x_i \right) / \Delta x_i.\end{aligned}$$

In this way, if we set $w_h = L_h(u)$, and $E_i(\psi) = \int_{I_i} \psi - \sum_{l=1}^L \omega_l \psi(x_{i,l}) \Delta x_i$, we have :

$$\begin{aligned}e_2(x) &= \mathbb{P}_h(-\partial_x f(u))(x) - L_h(u)(x) \\ &= [\tilde{v}_i - \bar{w}_i] \cdot [2(x - x_i) / \Delta x_i] \\ &= \left[-6 \left\{ \int_{I_i} f(u(x)) dx \right\} / (\Delta x_i)^2 + 6 \left\{ \sum_{l=1}^L \omega_l \cdot f(u(x_{i,l})) \right\} / \Delta x_i \right] \times \\ &\quad \times [2(x - x_i) / \Delta x_i] \\ &= -12(x - x_i) \left[\int_{I_i} f(u(x)) dx - \sum_{l=1}^L \omega_l \cdot f(u(x_{i,l})) \Delta x_i \right] / (\Delta x_i)^3 \\ &= -12(x - x_i) E_i(f(u)) / (\Delta x_i)^3.\end{aligned}$$

Now, using the theory of interpolation, see for example Ciarlet [5], we obtain easily

$$\begin{aligned}\|e_1\|_{L^\infty(I_i)} &\leq C (\Delta x_i)^2 \|\partial_x^3 f(u)\|_{L^\infty(I_i)}, \\ \|e_2\|_{L^\infty(I_i)} &\leq 6 (\Delta x_i)^{-2} \|E_i(f(u))\|_{L^\infty(I_i)} \\ &\leq C (\Delta x_i)^k \|\partial_x^{k+1} f(u)\|_{L^\infty(I_i)},\end{aligned}$$

assuming that the quadrature rule (2.5) is exact for polynomials of degree k . By hypothesis we can take $k = 2$. This proves the result. \square

Note that if the quadrature formula (2.5) is exact only for polynomials of degree one $L_h(u)$ becomes only a first-order accurate approximation of $-\partial_x f(u)$, unless, of course, if $f' \equiv \text{Cst}$.

3. THE TIME-DISCRETIZATION

Let $\{t^n\}_{n=1, \dots, nt}$ be a partition of $[0, T]$, set $\Delta t^n = t^{n+1} - t^n$, and let the CFL-number be defined by

$$\text{CFL} = \sup_{i \in \mathbb{Z}, n=1, \dots, N} \frac{\Delta t^n}{\Delta x_i} \cdot \|f'\|_{L^\infty(C(u_0))},$$

where $C(u_0)$ denotes the convex hull of the range of the initial data u_0 .

Let us introduce the operator H_h^n :

$$(3.1) \quad \begin{aligned} H_h^n: BV(\mathcal{C}) \cap L^1(\mathcal{C}) &\rightarrow V_h(\mathcal{C}), \\ u &\mapsto \mathbb{P}_h(u) + \Delta t^n \cdot L_h(u). \end{aligned}$$

We now discretize the ODE (2.7a) as indicated by Shu and Osher in [12]:

(3.2a) Set $u_h(t=0) = \mathbb{P}_h(u_0)$;

(3.2b) For $n = 0, \dots, nt-1$ obtain $u_h(t^{n+1})$ from $u_h(t^n)$ as follows:

- (1) Compute $w_h(t^{n+1}) = H_h^n(u_h(t^n))$;
- (2) Set $u_h(t^{n+1}) = \frac{1}{2}u_h(t^n) + \frac{1}{2}H_h^n(w_h(t^{n+1}))$.

Note that the timestep sizes are not necessarily equal. Note also that at each time step, $u_h(t^{n+1})$ is obtained from $u_h(t^n)$ by simply applying twice the operator H_h^n . This makes the algorithm very easy to code.

As it is very well known, this time discretization of the ODE (2.7a) is formally second-order accurate. This fact, together with Proposition 2.1, allows us to say that the method (3.2) is formally second-order accurate.

Let us we assume that $\Delta x_i \equiv h$, that $\Delta t^n \equiv \Delta t$, and that $f'(u) = \text{Cst}$. In this case the operator H_h^n , in this Subsection written simply H_h , is linear. The L^2 -stability of the iterative procedure defined by (3.2), $u_h(t^{n+1}) = \frac{1}{2}[Id + H_h \circ H_h](u_h(t^n))$, is a necessary condition for its stability. Indeed, if the method is L^2 -unstable it is then automatically L^p -unstable, $\forall p \in [1, \infty]$. The reciprocal of this statement is not necessarily true; see Geveci [6]. In what follows we display the necessary and sufficient condition under which L^2 -stability is achieved.

An iterative procedure $u_h(t^{n+1}) = A(u_h(t^n))$, $u_h(0) = \mathbb{P}_h(u_0)$ is said to be L^2 -stable if there exists a constant C independent of the discretization parameters and the initial data u_0 such that

$$\|u_h(t^n)\|_{L^2(\mathcal{C})} \leq C \cdot \|u_0\|_{L^2(\mathcal{C})},$$

for every $t^n \in [0, T]$. The iterative procedure $u_n(t^{n+1}) = H_h(u_h(t^n))$, which is formally second-order accurate in space and only first-order accurate in time for any fixed CFL-number, was proven to be L^2 -stable if and only if the extremely restrictive condition $\text{CFL} = O(h^{1/2})$ is satisfied; see [2, 3]. In our case the scheme is formally second-order accurate both in time and space, and we have a much more satisfactory result (see fig. 3.1a):

PROPOSITION 3.1 : *Let f be an affine function of u . Then, the method (3.2) is L^2 -stable if and only if $\text{CFL} \leq 1/3$.*

We shall omit the proof of this result, for it is long and tedious. The interested reader can see [2, 3] to have an idea of the main lines of it, in the simpler case treated therein.

Let A be the symbol of the operator H_h , and let Γ be the curve in the complex plane of its eigenvalues. The stability condition $\text{CFL} = O(h^{1/2})$ reflects the fact that, for any $\text{CFL} > 0$, there is a part of Γ that lies outside the unit disk and that its farthest point is at a distance of $O(\text{CFL}^3)$ from it. This part of Γ lies in a neighborhood of $z = 1$ (the fact that the point $z = 1$ lies in Γ reflects the fact that the scheme is consistent). In our case $\mathcal{A} = F(A) = \frac{1}{2} [Id + A^2]$ is the symbol of the new operator $\frac{1}{2} [Id + H_h \circ H_h]$ and the curve of its eigenvalues is $F(\Gamma) = \frac{1}{2} [1 + \Gamma^2]$. Note that the transformation F leaves the point $z = 1$ invariant, and that, by the preceding result, for $\text{CFL} \leq 1/3$, $F(\Gamma)$ lies entirely in the unit disk. Roughly speaking F pushes Γ into the unit circle, thus improving the stability of the scheme ; see figures 3.1a and 3.1b. We can then say that the application of the Runge-Kutta technique has a stabilizing effect.

Although we have $L^2(\mathcal{C})$ -stability of the method under a very mild CFL condition in the linear case, this does not ensure its $L^2(\mathcal{C})$ -stability in the nonlinear case. In order to render the scheme not only $L^2(\mathcal{C})$ -stable but $L^\infty(\mathcal{C}) \cap BV(\mathcal{C})$ -stable, without compromising its formal second-order accuracy, we are going to use the $\Lambda\Pi_h$ -projection.

4. THE LOCAL PROJECTION $\Lambda\Pi_h$

The $\Lambda\Pi_h$ -operator we are going to use is a simplified TVBM version — inspired on the TVB-technique introduced by Shu, [11] — of the $\Lambda\Pi_h$ -projection used by Chavent and Cockburn, [3]. Consider the function :

$$(4.1a) \quad \tilde{m}(a_1, a_2, \dots, a_n) = \begin{cases} a_1, & \text{if } |a_1| \leq Mh^2, \\ m(a_1, a_2, \dots, a_n), & \text{otherwise,} \end{cases}$$

where M is some positive parameter, and m is the well-known minmod-function :

$$(4.1b) \quad m(a_1, a_2, \dots, a_n) = \begin{cases} s \cdot \min_{1 \leq i \leq n} |a_i|, & \text{if } \text{sign}(a_1) = \text{sign}(a_2) = \dots = \text{sign}(a_n) = s, \\ 0, & \text{otherwise.} \end{cases}$$

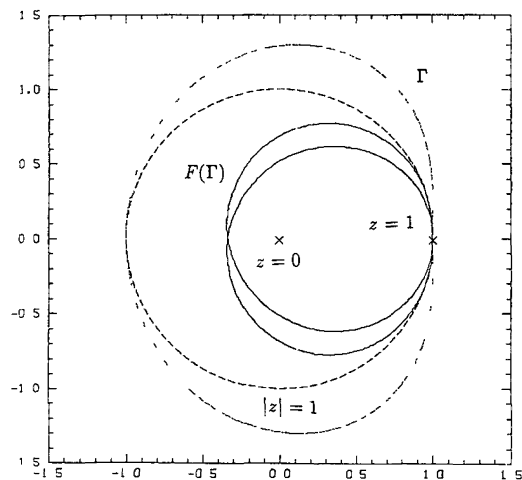


Figure 3.1a. — The curves Γ and $F(\Gamma) = \frac{1}{2} [1 + \Gamma^2]$ with $\text{CFL} = 1/3$.

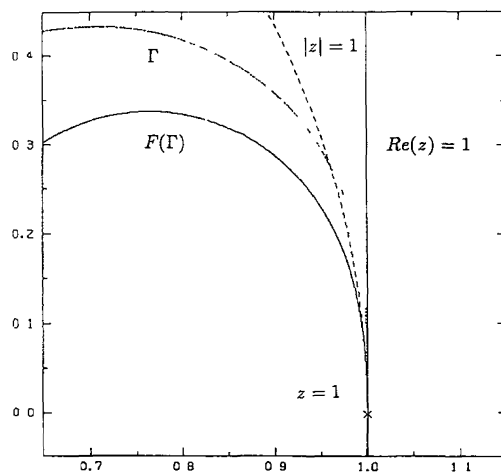


Figure 3.1b. — The curves Γ and $F(\Gamma) = \frac{1}{2} [1 + \Gamma^2]$ with $\text{CFL} = 1/9$ near $z = 1$.

We define the operator $\Lambda \Pi_h$ as follows :

$$(4.1c) \quad \begin{aligned} \Lambda \Pi_h : V_h(\mathcal{C}) &\rightarrow V_h(\mathcal{C}), \\ w_h &\mapsto w_h^*, \end{aligned}$$

where, the degrees of freedom of w_h^* are defined by :

$$(4.1d) \quad \begin{aligned} \bar{w}_i^* &= \bar{w}_i, \\ \tilde{w}_i^* &= \tilde{m}(\tilde{w}_i, \bar{w}_{i+1} - \bar{w}_i, \bar{w}_i - \bar{w}_{i-1}). \end{aligned}$$

The parameter M is a nonnegative real number whose purpose is to prevent the $\Lambda\Pi_h$ -projection of destroying the second-order accuracy of the scheme. This parameter is strongly related to the second derivative of the initial data u_0 , and will be estimated later. It was set equal to 0 for the $\Lambda\Pi P^0 P^1$ -scheme ; see [3].

The following result is a straightforward consequence of the definition of the $\Lambda\Pi_h$ -operator (4.1). We use the notation introduced above.

LEMMA 4.1 : *The $\Lambda\Pi_h$ -operator is a projection*

$$(1) \quad \Lambda\Pi_h(w_h^*) = w_h^* ;$$

satisfying the following global properties :

$$(2) \quad \bar{w}_h^* = \bar{w}_h ;$$

$$(3) \quad \int_{\mathcal{G}} w_h^* = \int_{\mathcal{G}} w_h ;$$

$$(4) \quad \|w_h^*\|_{L^\infty(\mathcal{G})} \leq \|\bar{w}_h\|_{L^\infty(\mathcal{G})} + M \cdot h^2 ;$$

$$(5) \quad \|\tilde{w}_h^*\|_{L^1(\mathcal{G})} \leq \frac{1}{2} h \cdot \|\bar{w}_h\|_{BV(\mathcal{G})} + M \cdot |\mathcal{G}| \cdot h^2.$$

Note that

$$\int_{\mathcal{G}} w_h^* = \int_{\mathcal{G}} \bar{w}_h^* = \int_{\mathcal{G}} \bar{w}_h = \int_{\mathcal{G}} w_h.$$

Thus, the $\Lambda\Pi_h$ -operator is a conservative (3), (local) projection (1), that leaves invariant the means (2). Properties (4) and (5) allow us to control $\Lambda\Pi_h(w_h)$ only in terms of \bar{w}_h . This is the key fact that will allow us to obtain the compactness of the sequence of approximate solutions generated by the $RK\Lambda\Pi P^1$ -scheme, as we shall see later.

Next, we show that when the solution of the conservation law is smooth enough, the application of the $\Lambda\Pi_h$ -projection does not destroy the already achieved accuracy of the scheme. We state this property in the following way :

LEMMA 4.2 : *Let u be an element of $C^2(\mathcal{G})$. Let \mathbb{P}_h be the L^2 -projection into $V_h(\mathcal{G})$. Then, there exists an $h_0 = h_0(u) > 0$ and an $M_0 = M_0(u)$ such that if $M \geq M_0$:*

$$\Lambda\Pi_h(\mathbb{P}_h(u)) = \mathbb{P}_h(u), \quad \forall h \leq h_0.$$

Proof : Let us assume that $u \in C^3(\mathcal{G})$, the extension of the proof to the case under consideration is straightforward. Let x be an arbitrary point of

\mathcal{C} , set $w_h = \mathbb{P}_h(u)$ and $w_h^* = \Lambda \Pi_h(w_h)$. By using Taylor expansion we can easily find that

$$\begin{aligned}\bar{w}_{i+1} - \bar{w}_i &= \left[\frac{\Delta x_{i+1} + \Delta x_i}{2} \right] \cdot \partial_x u(x) + O(h^2), \\ \bar{w}_i &= \left[\frac{\Delta x_i}{2} \right] \cdot \partial_x u(x) + \left[\frac{\Delta x_i}{2} (x_i - x) \right] \partial_{xx} u(x) + O(h^3).\end{aligned}$$

If $\partial_x u(x) \neq 0$ it is clear that for h small enough \bar{w}_i will lie in the interval $I(0, \bar{w}_i - \bar{w}_{i-1}) \cap I(0, \bar{w}_{i+1} - \bar{w}_i)$ for $i = 1, \dots, nx$. In this case we shall have $\tilde{w}^* = \tilde{w}$; see (4.1).

Now let us consider the case $\partial_x u(x) = 0$. Set $\mathcal{X} = \{x \in \mathcal{C} : \partial_x u(x) = 0, \partial_{xx} u(x) \neq 0\}$ and $\mathcal{J}_h^v = \{j : \text{the interval } I(x_j, x) \text{ is covered by at most } v \text{ intervals } I_i, \text{ where } x \in \mathcal{X}\}$. From the above expressions we see that for h small there is a constant independent of h, c_0 , such that $\max_{\{j \in \mathcal{J}_h^v\}} |\tilde{w}_j| \leq$

$c_0 \frac{v}{2} h^2 \sup_{\{x \in \mathcal{X}\}} |\partial_{xx} u(x)|$. Thus, in order to have $\tilde{w}_j^* = \tilde{w}_j$ for $j \in \mathcal{J}_h^v$ it is enough to take $M_0 = c_0 \frac{v}{2} \sup_{\{x \in \mathcal{X}\}} |\partial_{xx} u(x)|$. This proves the result. \square

We end this Section by noting that if the solution of (1.1) is always smooth, the absolute values of its second derivative at its extrema never increase. In this way if $M_0 = M_0(u_0)$ is such that $\Lambda \Pi_h(u_{0,h}) = u_{0,h}$ it is reasonable to expect that $\Lambda \Pi_h(u_h(t^n)) = u_h(t^n)$ for $n = 1, \dots, nt$.

5. THE $RK\Lambda\Pi P^1$ -METHOD

We can now define the $RK\Lambda\Pi P^1$ -method as follows :

(5.1a) Set $u_h(t = 0) = \mathbb{P}_h(u_0)$;

(5.1b) For $n = 0, \dots, nt - 1$ the approximate solution $u_h(t^{n+1})$ is obtained from u_h^n as follows :

(1) Compute $w_h(t^{n+1}) = \Lambda \Pi_h(H_h^n(u_h(t^n)))$;

(2) Set $u_h(t^{n+1}) = \Lambda \Pi_h\left(\frac{1}{2} u_h(t^n) + \frac{1}{2} H_h^n(w_h(t^{n+1}))\right)$;

Compare with algorithm (3.2). The stability and convergence properties of this scheme are based in the following key result.

LEMMA 5.1 : Let u_h be any element of the space $C_h(\mathcal{C}) = \Lambda \Pi_h(V_h(\mathcal{C}))$, and suppose that $h \cdot nx \leq C_0 |\mathcal{C}|$. Then, for $CFL \in [0, 1/2]$:

$$\|\overline{H}_h^n(u_h)\|_{BV(\mathcal{C})} \leq \|\bar{u}_h\|_{BV(\mathcal{C})} + C \cdot h,$$

where $C = 8 C_0 \cdot CFL \cdot M \cdot |\mathcal{C}|$.

Proof. Set $w_h = H_h^n(u_h)$. The means of w_h are given by :

$$\bar{w}_i = \bar{u}_i - (\Delta t^n / \Delta x_i) (f_{i+1/2}^G - f_{i-1/2}^G).$$

In order to rewrite this equation adequately, note that as $u_h \in C_h(\mathcal{C}) = \Lambda \Pi_h(V_h(\mathcal{C}))$ we have that $\tilde{u}_i = \mathbb{P}_{\mathbb{I}_{M,i}}(\tilde{u}_i)$; see (4.1c). Then, if we set

$$\begin{aligned}\tilde{v}_i &= \mathbb{P}_{\mathbb{I}_{(M-0),i}}(\tilde{u}_i), \\ r_i &= \tilde{u}_i - \tilde{v}_i,\end{aligned}$$

we have that $|r_i| \leq h^2 M$. Now, we rewrite this equation as follows :

$$\begin{aligned}\bar{w}_i &= \bar{u}_i + C_i(\bar{u}_{i+1} - \bar{u}_i) + D_i(\bar{u}_{i-1} - \bar{u}_i) \\ &\quad + A_i(-r_{i+1} + r_i) + B_i(r_{i-1} - r_i),\end{aligned}$$

where

$$\begin{aligned}A_i &= -\frac{\Delta t}{\Delta x_i} \cdot \frac{f^G(\bar{u}_{i+1} - \tilde{u}_{i+1}, \bar{u}_i + \tilde{u}_i) - f^G(\bar{u}_i - \tilde{u}_i, \bar{u}_i + \tilde{u}_i)}{(\bar{u}_{i+1} - \tilde{u}_{i+1}) - (\bar{u}_i - \tilde{u}_i)}, \\ B_i &= \frac{\Delta t}{\Delta x_i} \cdot \frac{f^G(\bar{u}_i - \tilde{u}_i, \bar{u}_i + \tilde{u}_i) - f^G(\bar{u}_i - \tilde{u}_i, \bar{u}_{i-1} + \tilde{u}_{i-1})}{(\bar{u}_{i-1} + \tilde{u}_{i-1}) - (\bar{u}_i + \tilde{u}_i)},\end{aligned}$$

and

$$\begin{aligned}C_i &= \left(1 - \frac{\tilde{v}_{i+1} - \tilde{v}_i}{\bar{u}_{i+1} - \bar{u}_i}\right) \cdot A_i, \\ D_i &= \left(1 + \frac{\tilde{v}_{i-1} - \tilde{v}_i}{\bar{u}_{i-1} - \bar{u}_i}\right) \cdot B_i.\end{aligned}$$

We only have to follow [3] in order to obtain :

$$\|\bar{w}_h\|_{BV(\mathcal{C})} \leq \|\bar{u}_h\|_{BV(\mathcal{C})} + 8 \max_i \{A_i^n, B_i^n\} \cdot \max_i \{|r_i|\} nx,$$

for $\text{CFL} \in [0, 1/2]$. Finally, as $\max_i \{A_i^n, B_i^n\} \leq \text{CFL}$, $\max_i \{|r_i|\} \leq h^2 M$,

and $nx \leq C_0 |\mathcal{C}| h^{-1}$ the result follows. \square

Let $\{u_h(t^n)\}_{n=0, \dots, nt}$ be the sequence generated by the $RK\Lambda\Pi P^1$ -method (5.1). Let us define its Q^1 -interpolate, denoted again by u_h , as follows :

$$u_h(t) = \left[\frac{t - t^n}{\Delta t^n} \right] u_h(t^{n+1}) + \left[\frac{t^{n+1} - t}{\Delta t^n} \right] u_h(t^n), \quad \forall t \in [t^n, t^{n+1}].$$

THEOREM 5.2 : Suppose that $\text{CFL} \in [0, 1/2]$, that $nx \cdot h \leq C_0 |\mathcal{C}|$, and that $nt \cdot h \leq C_1 T$. Let $\{u_h\}_{h \downarrow 0}$ be the sequence of Q^1 -interpolates of the

approximate solution defined by the $RK\Lambda\Pi P^1$ -method (5.1). Then

$$\begin{aligned}\|\bar{u}_h(t)\|_{BV(\mathcal{G})} &\leq \|u_0\|_{BV(\mathcal{G})} + C, \\ \|\tilde{u}_h(t)\|_{L^1(\mathcal{G})} &\leq h \cdot \left\{ \frac{1}{2} \|u_0\|_{BV(\mathcal{G})} + C \right\}, \quad \forall t \in [0, T],\end{aligned}$$

where $C = \max \{8 C_0 C_1 \cdot \text{CFL} \cdot M \cdot T \cdot |\mathcal{G}|, 2 M \cdot |\mathcal{G}| \cdot h\}$. In other words, the scheme is TVB.

Proof: It is enough to prove these inequalities for $t = t^n$. Since $u_h(t^{n+1}) = w_h^* = \Lambda\Pi_h(w_h)$, with $w_h = \frac{1}{2} u_h(t^n) + \frac{1}{2} H_h^n(\Lambda\Pi_h(H_h^n(u_h(t^n))))$, the second inequality is obtained easily from the first one:

$$\begin{aligned}\|\tilde{u}_h(t^{n+1})\|_{L^1(\mathcal{G})} &= \|\tilde{w}_h^*\|_{L^1(\mathcal{G})} \\ &\leq \frac{1}{2} h \cdot \|\bar{w}_h\|_{BV(\mathcal{G})} + M \cdot |\mathcal{G}| \cdot h^2, \text{ by (5), Lemma 4.1,} \\ &= \frac{1}{2} h \cdot \|\bar{w}_h^*\|_{BV(\mathcal{G})} + M \cdot |\mathcal{G}| \cdot h^2, \text{ by (2), Lemma 4.1,} \\ &\leq \frac{1}{2} h \cdot \|\bar{u}_h(t^{n+1})\|_{BV(\mathcal{G})} + \frac{1}{2} C.\end{aligned}$$

The first one is obtained as follows:

$$\begin{aligned}\|\bar{u}_h(t^{n+1})\|_{BV(\mathcal{G})} &= \|\bar{w}_h^*\|_{BV(\mathcal{G})} \\ &= \left\| \frac{1}{2} \bar{u}_h(t^n) + \frac{1}{2} \bar{H}_h^n(\Lambda\Pi_h(H_h^n(u_h(t^n)))) \right\|_{BV(\mathcal{G})} \\ &\leq \frac{1}{2} \left[\|\bar{u}_h(t^n)\|_{BV(\mathcal{G})} + \|\bar{H}_h^n(\Lambda\Pi_h(H_h^n(u_h(t^n))))\|_{BV(\mathcal{G})} \right] \\ &\leq \frac{1}{2} \left[\|\bar{u}_h(t^n)\|_{BV(\mathcal{G})} + \|\bar{H}_h^n(u_h(t^n))\|_{BV(\mathcal{G})} + C' \cdot h \right],\end{aligned}$$

by Lemma 5.1, and (2), Lemma 4.1,

$$\leq \frac{1}{2} \left[\|\bar{u}_h(t^n)\|_{BV(\mathcal{G})} + \|\bar{u}_h(t^n)\|_{BV(\mathcal{G})} + 2 C' \cdot h \right],$$

again by Lemma 5.1,

$$\begin{aligned}&\leq \|\bar{u}_h(t^n)\|_{BV(\mathcal{G})} + C' \cdot h, \\ &\leq \|\bar{u}_{0,h}\|_{BV(\mathcal{G})} + C' \cdot nt \cdot h, \\ &\leq \|u_0\|_{BV(\mathcal{G})} + C' \cdot C_1 \cdot T, \text{ by hypothesis.}\end{aligned}$$

The result follows from the fact that $C' = 8 C_0 \cdot \text{CFL} \cdot M \cdot |\mathcal{G}|$; see Lemma 5.1. \square

COROLLARY 5.3 : Suppose the hypothesis of the preceding Theorem are verified. Then, there is a subsequence of the sequence $\{u_h\}_{h \downarrow 0}$ generated by the $RK\Lambda\Pi P^1$ -method (5.1) which converges to a weak solution of (1.1).

Proof : By Theorem 5.2 there is a subsequence $\{u_{h'}\}_{h' \downarrow 0}$ that converges in $L^\infty(0, T; L^1(\mathcal{C}))$ to a function $u^* \in L^\infty(0, T; L^1(\mathcal{C}) \cap BV(\mathcal{C}))$. Let us think of the functions \tilde{u}_h as already known parameters that tend to 0 in $L^\infty(0, T; L^1(\mathcal{C}))$, and let us consider the scheme (5.1) as a scheme only for the means \bar{u}_h . It can be easily seen that this scheme is a conservative scheme whose numerical flux is consistent with f . Thus, as $\bar{u}_{h'} \rightarrow u^*$, by Theorem (5.2), the limit u^* must be a weak solution of (1.1) by the well known Lax-Wendroff Theorem [8]. This proves the result. \square

6. NUMERICAL RESULTS

In this section we test the $RK\Lambda\Pi P^1$ -method in six different problems (1.1) for which we can calculate the exact solution. Our test problems are defined by giving the circle \mathcal{C} (that we identify with the interval $[0, l)$), the final time T , the nonlinearity f , and the initial data u_0 on Ω ; see table 6.1. Their corresponding exact solutions are displayed on figure 6.1. On table 6.2 we define the sets \mathcal{C}' on which the entropy solution u can be considered smooth. They have been obtained from \mathcal{C} by subtracting subsets that contain discontinuities of either u or $\partial_x u$.

TABLE 6.1
Definition of the test problems.

| Problem | \mathcal{C} | T | $f(u)$ | $u_0(x)$ |
|---------|---------------|---|---|---|
| 1 | $[0, 1)$ | 0.15 | u | $\frac{1}{2} \left(1 + \frac{1}{2} \sin (4 \pi x) \right)$ |
| 2a | $[0, 1)$ | $\left\{ \begin{array}{l} 0.15 \\ 1/\pi \end{array} \right\}$ | $u^2/2$ | $\frac{1}{2} \left(\frac{1}{2} + \sin (2 \pi x) \right)$ |
| 2b | | | | |
| 2c | $[0, 1)$ | 0.1 | $\frac{1}{2} \frac{u^2}{u^2 + (1 - u)^2}$ | $\frac{1}{2} \left(1 + \frac{1}{2} \sin (4 \pi x) \right)$ |
| 3 | | | | |
| 4 | $[0, 1)$ | 0.15 | u | $\begin{cases} 1, & \text{if } x \in (0.4, 0.6), \\ 0, & \text{otherwise.} \end{cases}$ |
| 5 | $[0, 2)$ | 0.5 | $u(1 - u)$ | $\begin{cases} 1, & \text{if } x \in (0.5, 1.5), \\ 0, & \text{otherwise.} \end{cases}$ |
| 6 | $[0, 2)$ | 0.5 | $\frac{1}{2} \frac{u^2}{u^2 + (1 - u)^2}$ | $\begin{cases} 1, & \text{if } x \in (0.5, 1.5), \\ 0, & \text{otherwise.} \end{cases}$ |

TABLE 6.2

Definition of the domains \mathcal{C}' on which $u(T)$ is smooth.

| Problem | \mathcal{C}' | Singularities of $u(T)$ |
|---------|--|--|
| 1 | $[0, 1)$ | none |
| 2a | $[0, 1)$ | none |
| 2b | $[0, 0.04] \cup [0.14, 1)$ | shock appears near $x = 0.08$ |
| 2c | $[0, 0.09] \cup [0.19, 1)$ | shock near $x = 0.14$ |
| 3 | $[0, 1)$ | none |
| 4 | $[0, 0.5] \cup [0.6, 0.7] \cup [0.8, 1)$ | two contact disc. at $x = 0.55, 0.75$ |
| 5 | $[0.05, 0.45] \cup [0.55, 0.95] \cup [1.05, 1.95]$ | stationary shock at $x = 0.5$, two disc. of $\partial_x u$ at $x = 1, 2$. |
| 6 | $[0, 0.75] \cup [0.85, 1.75] \cup [1.85, 2)$ | two shocks near $x = 0.8, 1.8$ |

The quadrature rule (2.5) used in these computations is the three-point Gauss rule. Although Corollary 5.3 ensures the convergence of the method for $\text{CFL} \in [0, 1/2]$, Proposition 3.1 guarantees L^2 -stability only for $\text{CFL} \in [0, 1/3]$ in the linear case. This is why we are going to perform our computations with $\text{CFL} = 1/3$. On table 6.3 we display the $L^1(\mathcal{C}')$ -errors,

TABLE 6.3

L^1 -errors and orders of convergence for $\text{CFL} = 1/3$. The quantity e_1 is equal to $\|u(T) - u_h(T)\|_{L^1(\mathcal{C}')}$, and α_1 is the corresponding order of convergence. For all the tests we have taken $\Delta x = \frac{1}{200}$. The sets \mathcal{C}' are defined in table 6.2.

| Problem | No projection | | $M \equiv 0$ | | $M \cdot h^2 = \mathcal{M}_0$ | |
|---------|------------------|------------|------------------|------------|-------------------------------|------------|
| | $10^4 \cdot e_1$ | α_1 | $10^4 \cdot e_1$ | α_1 | $10^4 \cdot e_1$ | α_1 |
| 1 | 0.57 | 1.97 | 1.28 | 2.24 | 0.57 | 1.97 |
| 2a | 0.21 | 1.96 | 0.34 | 2.11 | 0.21 | 1.96 |
| 2b | 0.09 | 2.01 | 0.30 | 2.25 | 0.09 | 2.01 |
| 2c | 0.02 | 2.00 | 0.02 | 2.00 | 0.02 | 2.00 |
| 3 | 0.87 | 1.94 | 1.25 | 2.06 | 0.87 | 1.94 |
| 4 | 21.4 | 1.00 | 0.0004 | — | 0.0004 | — |
| 5 | 7.20 | 1.13 | 6.19 | 0.99 | 6.19 | 0.95 |
| 6 | 248 | 0.002 | 0.39 | 0.99 | 0.39 | 0.99 |

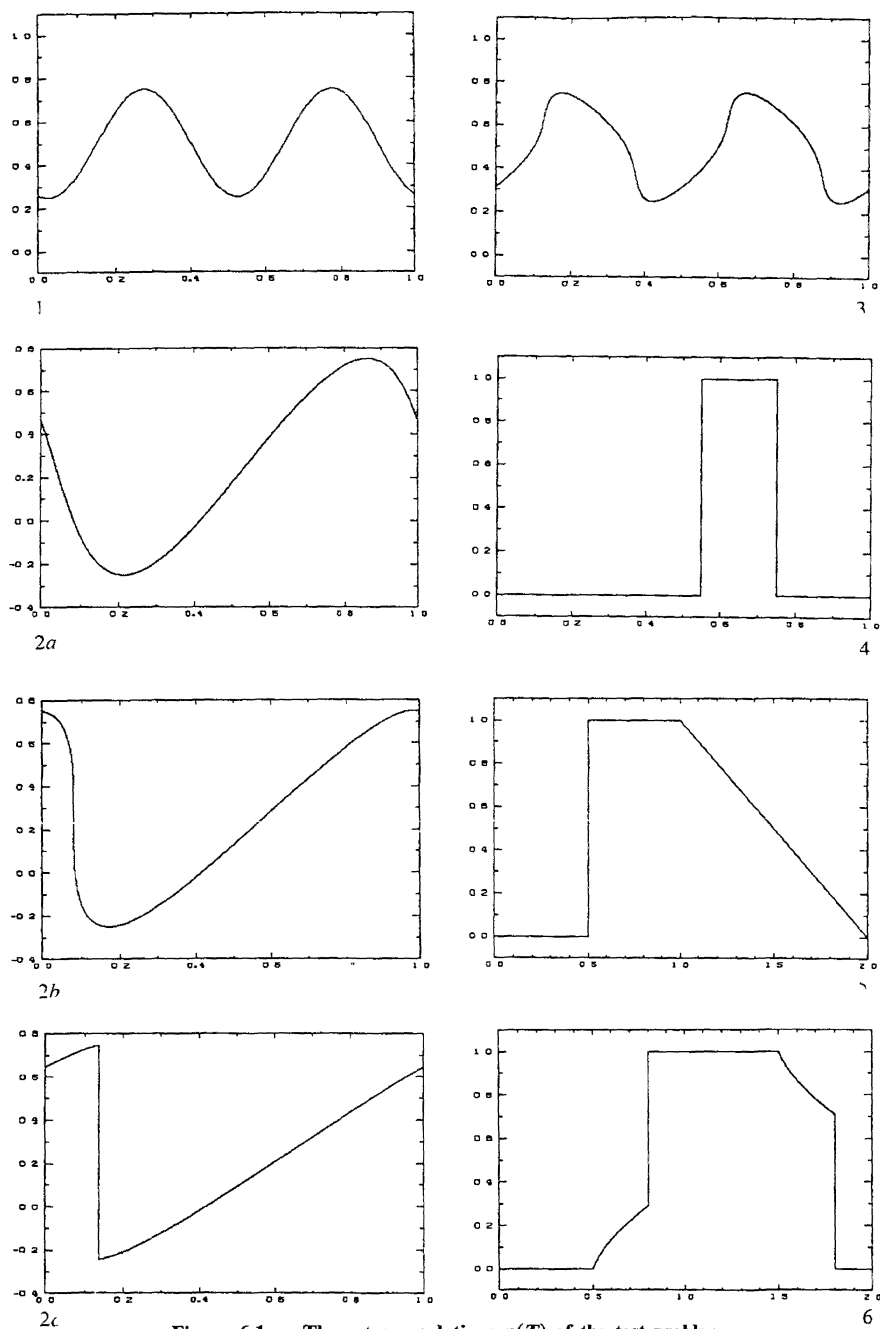


Figure 6.1. — The entropy solutions $u(T)$ of the test problems.

and on table 6.4 the $L^\infty(\mathcal{C}')$ ones. Details of how the discontinuities are captured are shown on figures 6.3, 6.4 and 6.5.

In table 6.3, some of the results corresponding to problem 4 have not been included, for in this case a superconvergence, that is far from being typical, is observed. This is due to the facts that, on \mathcal{C}' , we have $\partial_x^n u \equiv 0$, $\forall n \geq 1$, and that the approximate solution does not oscillate! When the projection is not used, strong oscillations away of the discontinuities appear. They travel faster than the discontinuities. See figures 6.2.

The results on table 6.3 and table 6.4 show that L^1 -second-order accuracy has been obtained for test problems 1, 2 and 3, regardless of the values of M . Uniform second-order accuracy away from discontinuities has also been obtained. Notice that for M small enough the $\Lambda\Pi_h$ -projection is not equal to the identity, and its application produces loss of accuracy only near the extrema. In fact we can notice that :

- 1) the influence of the $\Lambda\Pi_h$ -projection appears only in the presence of extrema because in problem 2c (for which the entropy solution does not have extrema but two smooth monotone regions between the shocks) the results are independent of the value of M (the value of M for problems 4, 5 and 6 is zero) ;
- 2) this loss of accuracy is indeed of a local character. Consider the problems 1, 2a, b and 3, which are the only ones with a solution with extrema. Note, on tables 6.4 and 6.5, how the loss of accuracy is greater

TABLE 6.4

L^∞ -errors and orders of convergence for CFL = 1/3. The quantity e_∞ is equal to $\|u(T) - u_h(T)\|_{L^\infty(\mathcal{C}')}$, and α_∞ is the corresponding order of convergence. For all the tests we have taken $\Delta x = \frac{1}{200}$. The sets \mathcal{C}' are defined in table 6.3.

| Problem | No projection | | $M \equiv 0$ | | $M \cdot h^2 = 0$ | |
|---------|---------------------|-----------------|------------------|------------|---------------------|------------|
| | $10^4 \cdot e_\tau$ | α_∞ | $10^4 \cdot e_x$ | α_x | $10^4 \cdot e_\tau$ | α_x |
| 1 | 1.56 | 1.94 | 10.1 | 1.55 | 1.56 | 1.94 |
| 2a | 1.28 | 1.98 | 5.04 | 1.24 | 1.28 | 1.98 |
| 2b | 1.22 | 2.04 | 6.51 | 1.71 | 1.22 | 2.04 |
| 2c | 0.15 | 1.81 | 0.15 | 1.80 | 0.15 | 1.81 |
| 3 | 10.5 | 1.95 | 10.5 | 1.95 | 10.5 | 1.95 |
| 4 | 199.4 | 1.16 | 0.05 | — | 0.05 | — |
| 5 | 24.15 | 1.82 | 16.41 | 0.96 | 16.41 | 0.96 |
| 6 | 1966 | 0.08 | 2.63 | 1.06 | 2.63 | 1.06 |

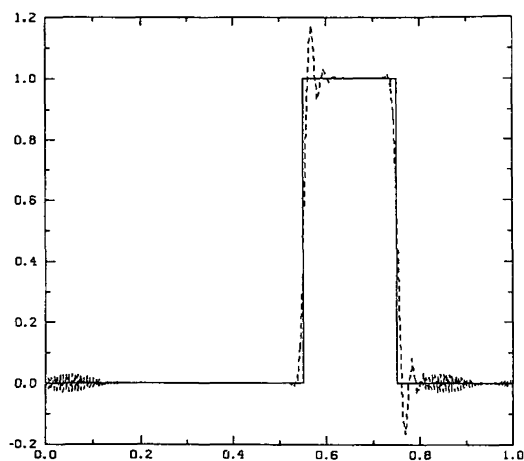


Figure 6.2a. — Test problem 4 without the $\Lambda\Pi_h$ -projection: f linear, $\text{CFL} = 1/3$, $\Delta x = \frac{1}{200}$. (The solid line represents the exact solution, and the dashed one the approximate solution.)

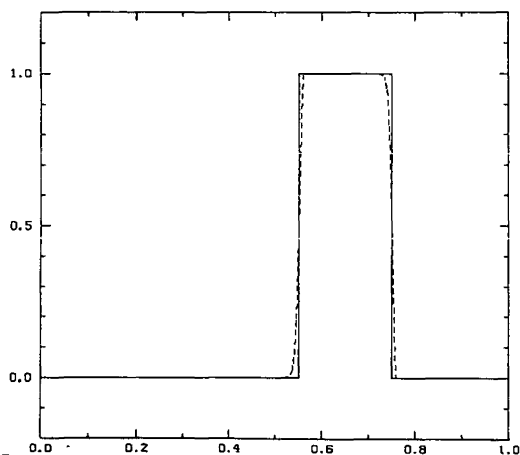


Figure 6.2b. — Test problem 4 with the $\Lambda\Pi_h$ -projection: f linear, $\text{CFL} = 1/3$, $\Delta x = \frac{1}{200}$.

when $M \equiv 0$, and how in this case the order of convergence is lowered dramatically for the L^∞ norm while the order of convergence for the L^1 norm remains the same. (This cannot be seen for problem 3 because the maximum error is attained not at the extrema but at some points between them at which the function $|\partial_x u|$ becomes very big !);

3) for « big » values of M the $\Lambda\Pi_h$ -projection reduces to the identity.

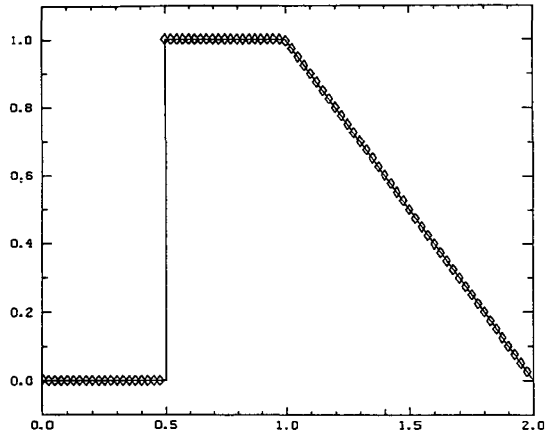


Figure 6.3a. — Test problem 5 : f concave, $\text{CFL} = 1/3$, $\Delta x = \frac{1}{200}$. (The solid line represents the exact solution. A \diamond is placed at $(x_{i+1/2}, u_h(x_{i+1/2}))$ every five elements.)

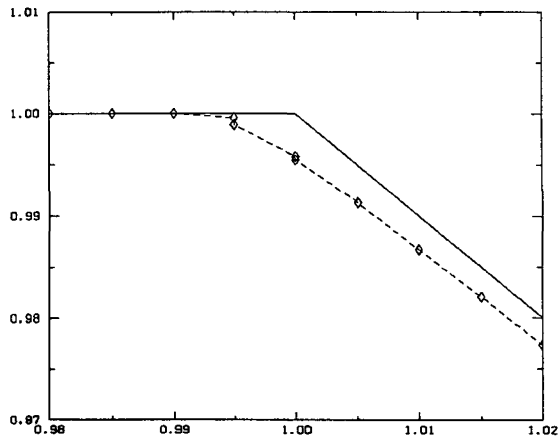


Figure 6.3b. — Test problem 5 : Zoom on figure 6.3a. (The solid line represents the exact solution. The dashed line joining the \diamond represents the approximate solution u_h .)

In problems 4, 5 and 6 (for which the initial data presents a discontinuity) we see that the introduction of the $\Lambda\Pi_h$ -projection (i) improves the accuracy of the method and (ii) enforces the convergence to the entropy solution. The most dramatic case is, of course, problem 6 (the nonlinearity f is nonconvex) for which the scheme without projection does not converge to the entropy solution.

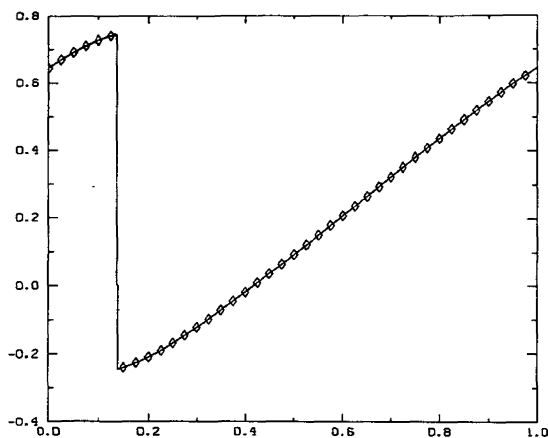


Figure 6.4a. — Test problem 2c: f convex, $\text{CFL} = 1/3$, $\Delta x = \frac{1}{200}$.

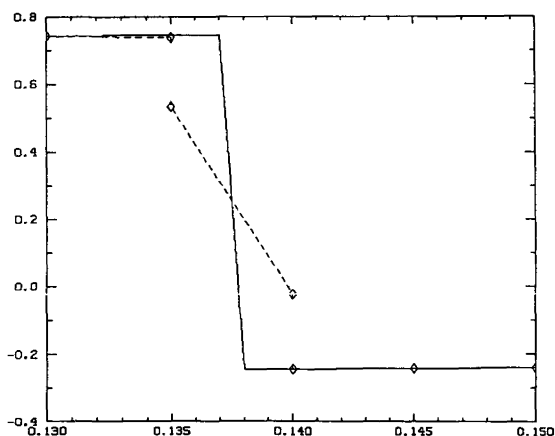


Figure 6.4b. — Test problem 2c: Zoom on figure 6.4a.

All these calculations have been redone for $\text{CFL} = 1/6$ with identical results. The influence of the decrease of CFL-number was negligible.

7. CONCLUDING REMARKS

In this paper we have introduced, analyzed, and tested numerically the $RK\Lambda PP^1$ -method, which is the model scheme of a new class of schemes devised to solve numerically hyperbolic conservation laws (1.1). The scheme is constructed as follows :

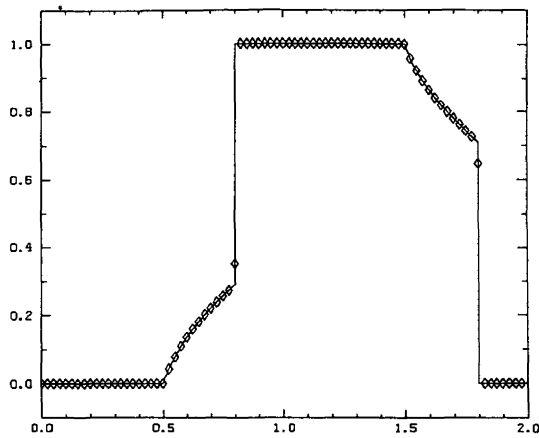


Figure 6.5a. — Test problem 3 : f nonconvex, $CFL = 1/3$, $\Delta x = \frac{1}{200}$.

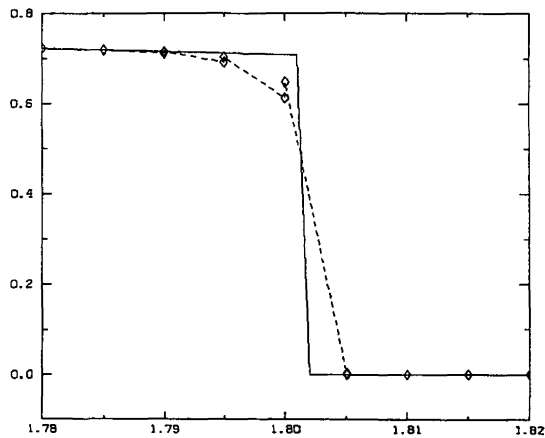


Figure 6.5b. — Test problem 3 : Zoom on figure 6.5a.

- 1) the Discontinuous-Galerkin Method, as employed in [3, 4], is used to discretize in space the conservation law,
- 2) a TVD time discretization [12] is used to discretize the so-obtained ODE,
- 3) a local projection which enforces stability without destroying the already achieved accuracy is applied at each intermediate stage of the Runge-Kutta method.

We proved that the resulting scheme verifies a maximum principle, that it is total variation bounded in the means, formally uniformly second-order accurate, and that it converges to a weak solution. Without the projection, the scheme is linearly stable if $\text{CFL} \leq 1/3$.

Our numerical results indicate that, for $\text{CFL} \leq 1/3$, the $RK\Lambda\text{IIP}^1$ -method is a stable method that converges to the entropy solution, even for nonconvex nonlinearities f . In smooth regions of the entropy solution the method was found to be uniformly second-order accurate away from the discontinuities when the initial data was smooth, and was able to capture shocks, essentially, within a single element. The method is easy to code, and its construction does not depend on the type of nonlinearity f under consideration.

The three principles with which our model scheme has been constructed can be also used to define numerical schemes in a more general setting. Higher-order versions of this method, as well as extensions to the nonperiodic case, systems and the multidimensional case, constitute the object of work in progress.

REFERENCES

- [1] Y. BRENIER and S. OSHER, *Approximate Riemman Solvers, and Numerical Flux Functions*, ICASE-NASA Langley Center report n° 84-63, Hampton, VA, 1984.
- [2] G. CHAVENT and B. COCKBURN, *Consistance et Stabilité des Schémas LRG pour les Lois de Conservation Scalaires*, INRIA report # 370 (1987).
- [3] G. CHAVENT and B. COCKBURN, *The Local Projection Discontinuous Galerkin Finite Element Method for Scalar Conservation Laws*, *M²AN*, 23 (1989), pp. 565-592.
- [4] G. CHAVENT and G. SALZANO, *A Finite Element Method for the 1D Water Flooding Problem with Gravity*, *J. Comput. Phys.*, 45 (1982), pp. 307-344.
- [5] P. G. CIARLET, *The Finite Element Method for Elliptic Problems*, North Holland, 1975.
- [6] T. GEVECI, *The Significance of the Stability of Difference Schemes in Different l^p -spaces*, *SIAM Review*, 24 (1982), pp. 413-426.
- [7] B. A. FRYXEL, P. R. WOODWARD, P. COLLELA and K. H. WINKLER, *An Implicit-Explicit Hybrid Method for Lagrangian Hydrodynamics*, *J. Comput. Phys.*, 63 (1986), pp. 283-310.
- [8] P. D. LAX and B. WENDROFF, *Systems of Conservation Laws*, *Comm. Pure and Appl. Math.*, 13 (1960), pp. 217-237.
- [9] S. OSHER, *Riemman Solvers, the Entropy Condition, and Difference Approximations*, *SIAM J. Numer. Anal.*, 21 (1984), pp. 217-235.

- [10] B. VAN LEER, *Towards the Ultimate Conservative Scheme, VI. A New Approach to Numerical Convection*, J. Comput. Phys., 23 (1977), pp. 276-299.
- [11] C. W. SHU, *TVB uniformly high-order schemes for conservation laws*, Math. Comp., 49 (1987), pp. 105-121.
- [12] C. W. SHU and S. OSHER, *Efficient Implementation of Essentially Non-Oscillatory Shock-Capturing Schemes*, J. Comput. Phys., 77 (1988), pp. 439-471.